Available online at www.sciencedirect.com

SCIENCE DIRECT®

Cement and Concrete Research 35 (2005) 513–519

CEMENT AND CONCRETE RESEARCH

Evaluation of capillary pore size characteristics in high-strength concrete at early ages

Shin-ichi Igarashi*, Akio Watanabe, Mitsunori Kawamura

Department of Civil Engineering, Kanazawa University, 2-40-20 Kodatsuno, Kanazawa 920-8667, Japan

Received 26 February 2001; accepted 29 June 2004

Abstract

The quantitative scanning electron microscope-backscattered electron (SEM-BSE) image analysis was used to evaluate capillary porosity and pore size distributions in high-strength concretes at early ages. The Powers model for the hydration of cement was applied to the interpretation of the results of image analysis. The image analysis revealed that pore size distributions in concretes with an extremely low water/binder ratio of 0.25 at early ages were discontinuous in the range of finer capillary pores. However, silica-fume-containing concretes with a water/binder ratio of 0.25 had larger amounts of fine pores than did concretes without silica fume. The presence of larger amounts of fine capillary pores in the concretes with silica fume may be responsible for greater autogenous shrinkage in the silica-fume-containing concretes at early ages.

Keywords: Backscattered electron imaging; Microstructure; Pore size distribution; Shrinkage; Silica fume

1. Introduction

High-strength concretes with extremely low water/cement ratios undergo significant self-desiccation if no external water is supplied to the concrete during the initial hydration process. Self-desiccation results in remarkable autogenous shrinkage, which may cause cracks in the premature concretes. Therefore, the properties of mature high-strength concrete with an extremely low water/cement ratio may be sensitive to the initial curing condition, compared with that of ordinary concretes with relatively high water/cement ratios [1]. However, the effects of insufficient water supply on the formation of the microstructure in high-strength concretes at early ages have not been fully understood. Taking into account that the autogenous shrinkage at early ages is usually explained by the evolution of capillary tension, it is significant for the better understanding of the nature of autogenous shrinkage to reveal the characteristics of capillary pore structures in high-strength concretes at early ages.

To investigate pore structures in cementitious materials, the mercury intrusion porosimetry (MIP) method has been used for many years. The results obtained from the MIP method suggest that large capillary pores are more significant in determining the mechanical properties and permeability of concrete. The MIP measurements also showed that the total volume as well as the distribution and connectivity of pores were significant to control various properties of concretes. However, it has been criticized that the features of pore structure characterized by the MIP method are not representative of the real pore structure because of improper assumptions made on the shape of the pores and their connectivity in concrete in the method [2]. Furthermore, in terms of practical experimental procedures, cement paste samples used in the MIP measurements must be dried in advance. Therefore, strictly speaking, the pore structures characterized by the MIP

* Corresponding author.
E-mail address: igarashi@t.kanazawa-u.ac.jp (S. Igarashi).

0008-8846/$ - see front matter © 2004 Elsevier Ltd. All rights reserved.
doi:10.1016/j.cemconres.2004.06.036

method cannot be directly related to the shrinkage behaviors of cement paste.

An alternative method to characterize pore structures in concrete is the scanning electron microscope-backscattered electron (SEM-BSE) image analysis technique. Taking advantage of its usefulness and wide applicability as a quantitative method, pore structures in cement pastes and concretes have been evaluated by this imaging technique [3]. The sizes of pore diameters detected by this method are much greater than those by the MIP method. However, as mentioned above, the volume of coarse pores quantified by the imaging may play a significant role in various properties of concrete. Furthermore, area fractions of unhydrated cement particles evaluated by the imaging method can be related to the degree of hydration, which is an important parameter to characterize the hydration process [4,5]. Therefore, the SEM-BSE imaging technique can be expected to provide useful information for interpreting the behavior of concrete in terms of the evolution of microstructure at early ages.

The purpose of this study is to examine capillary pores and solid structures formed in high-strength concretes during the first 24 h after casting. Quantitative SEM-BSE image analyses were made to evaluate the coarse capillary porosity, pore size distributions and the degree of hydration in concretes with an extremely low water/binder ratio of 0.25. We tried to interpret the results in terms of the Powers model for the hydration of cement. The effects of an extremely low water/binder ratio of 0.25 and the addition of silica fume on the characteristics of the microstructure are also discussed, relating them to the tendency of autogenous shrinkage in high-strength concretes at early ages.

2. Experimental

2.1. Materials and mix proportion of concretes

The cement used was ordinary Portland cement. Its chemical compositions and physical properties are given in Table 1. A commercial silica fume with a specific surface area of 20 m^2/g was used. The replacement of silica fume for cement was 10 mass%. A river gravel with a maximum size of 10 mm was used as a coarse aggregate. The fine aggregate was a river sand from the same river as the coarse aggregate. Polycarboxylic acid superplasticizer was used. The water/binder ratio of concretes was 0.25. The mix proportions of the concretes are given in Table 2.

2.2. BSE image analysis

Concrete cylinders of 100 mm in length and 50 mm in diameter were produced. They were sealed immediately after casting and stored at 18 °C. At the age of 12 and 24 h, slices with about 10-mm thickness were cut from the central portions of the specimens. They were dried by ethanol replacement and then impregnated with the epoxy resin. After the resin had hardened at room temperature, the slices were carefully polished with silicon carbide papers (approximately 4 μm). Then, the polished surfaces were meticulously finished with diamond slurry (3, 1 and 0.25 μm) for a short time.

The specimens were examined using the SEM equipped with a quadruple backscatter detector. The BSE images were acquired at the magnification of ×500 by the use of high-resolution acquisition system. To avoid influences of interfacial transition zones around fine aggregate particles on the results, regions of interest for acquiring images in concretes were sufficiently away from the surfaces of the sand particles. It is, of course, probable that a region taken well away from a visible aggregate surface in a 2D image is either right above or right below another aggregate surface that is not visible in the image. However, such a 3D stereological aspect was not taken into account in this study. Each image consists of 1148×1000 pixels, with 1 pixel representing about 0.22×0.22 μm at that magnification. A dynamic thresholding method [6] for several neighbors of pixels was used to obtain the binary images of pores and unhydrated cement grains. In this method, the gray level histogram for the whole image as well as the local information on brightness at neighbor pixels are used to determine the threshold values for each pixel.

To extract the features of pore size distributions from a binary image, the equivalent diameter of a pore was used as a geometric measure [7,8]. Each pore cluster with irregular shape was labeled by the rule of eight-neighbor connectivity. The labeled pore clusters whose areas are tallied by pixels are converted to the equivalent circles with the same area as the original pores. Then, all the circle clusters were scaled by their diameters. The cumulative pore volume versus the equivalent diameter curves were plotted by sorting and cumulating the areas of those scaled circles. This procedure is essentially the same as the assumption of unit thickness for cylindrical pores representing the original pore cluster. However, it should be noted that large areas of pores are also derived from long continuous pores. Namely, the pore size distribution curve

Table 1
Chemical and physical properties of cement

Oxide composition (wt.%)									Loss on ignition (%)	Density (g/cm^3)
SiO_2	Al_2O_3	Fe_2O_3	CaO	MgO	SO_3	Na_2O	K_2O	Cl		
20.55	5.21	2.44	65.86	0.91	2.33	0.27	0.41	0.006	1.19	3.15

Table 2
Mix proportion of concretes

	W/B	Unit content (kg/m^3)					SP (wt.% of binder)
		Water	Cement	Silica fume	Sand	Gravel	
PC	0.25	145	581	0	559	1086	1.7
SF	0.25	142	510	57	559	1086	2.6

SP: superplasticizer.

obtained by the image analysis can reflect not only the quantity of pore with a specific size but also the continuity of capillary pores from a qualitative geometric perspective, because a 2D section is exposed from a 3D random isotropic material.

2.3. Calculation of volume fractions of constituent phases

The volume fractions of the constituent phases in cement pastes can be calculated using a model for the hydration of cement. In this study, the Powers model [9] was applied to the results of the image analysis [10]. In the calculation, the volume of cement gel produced by the hydration of 1 cm^3 dry cement was assumed to be 2.1 cm^3. The nonevaporable water content in the reacted cement is about 23 mass%. Chemical shrinkage was also assumed to be 0.254 of the volume of nonevaporable water. The porosity of cement gel used in the calculation was 28%, those pores saturated with gel water. The degree of hydration was determined by Eq. (1) [4,5].

$$\alpha = 1 - \frac{UH_i}{UH_0} \quad (1)$$

where UH_i is the area fraction of unhydrated cement particles at the age of t_i and UH_0 is the initial area fraction of unhydrated cement particles (i.e., t_i=0).

Based on the stereology principles, area fractions in 2D cross-sections are assumed to represent 3D volume fractions in a real porous material [11]. The volume fractions of the hydration products (i.e., CSH and calcium hydroxide crystals) were estimated using the degree of hydration and the Powers model. For example, if the value of 2.5 nm is assumed as the lower limit of size for capillary pores [12], the total volume of capillary pores greater than 2.5 nm in diameter was obtained by subtracting the volume of unhydrated cement and the calculated volume of cement gel from the initial volume of the mixture. Thus, the difference between the capillary pore volume calculated based on the Powers model and the coarse pore volume obtained by the image analysis represents the volume of fine pores whose diameters are less than the resolution of the image analysis (0.2 μm in this study). In this study, hereafter, capillary pores whose diameters are less than the resolution of the image analysis (i.e., range from 2.5 nm to 0.2 μm) are defined as “fine capillary pores”. Correspondingly, the pores tallied in the image analysis are termed “coarse capillary pores”. An example of BSE micrograph for the cement paste phase in concretes is given in Fig. 1.

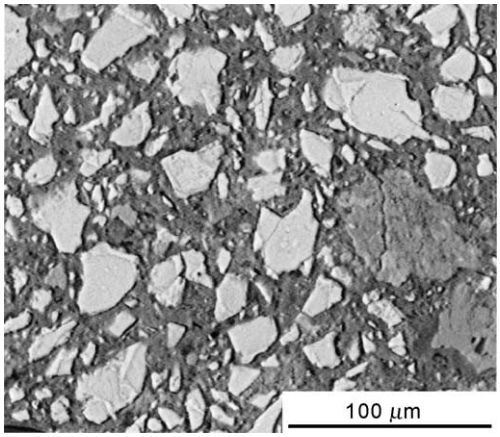

Fig. 1. BSE image for ordinary Portland cement concrete with a water/binder ratio of 0.25 at 24 h.

3. Results

3.1. Capillary porosity and pore size distributions

Fig. 2 shows the coarse capillary pore size distributions for the cement paste phase in high-strength concretes with and without silica fume. Silica-fume-containing concretes are found to have fewer coarse pores than do ordinary concretes, even at early ages of 12 and 24 h. The threshold diameter at which porosity starts to steeply increase with decreasing pore diameter is smaller in silica-fume-containing concretes than in ordinary concretes at 12 h. This smaller threshold diameter in silica-fume-containing concretes indicates higher packing density of binder grains in the concretes.

The difference in the initial porosity between ordinary concrete and 10% silica-fume-containing concrete is quite small by volume, as can be easily calculated using the densities of silica fume (2.2 g/cm^3) and ordinary Portland cement (3.15 g/cm^3). Furthermore, it has been pointed out that the total porosity estimated by the MIP method is not notably changed by the addition of silica fume at a given water/binder ratio [13,14]. Therefore, if there were little differences in the total porosity between concretes with and without silica fume at early ages also, the difference

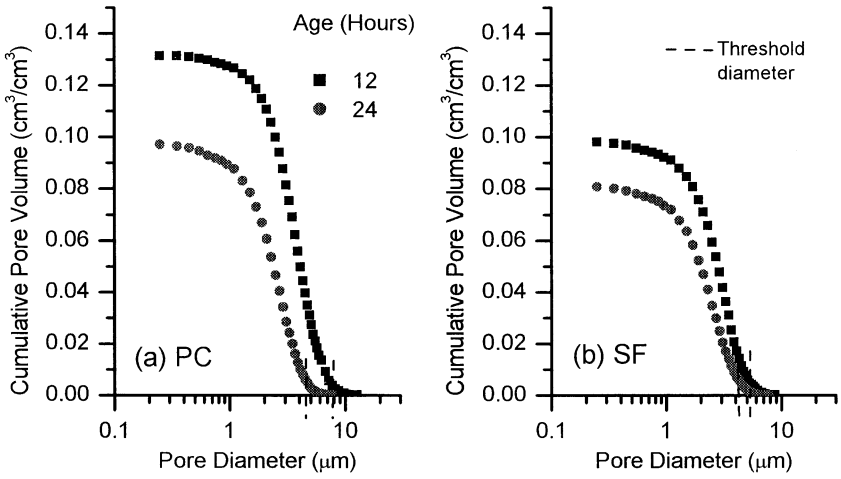

Fig. 2. Coarse capillary pore size distributions at early ages: (a) Portland cement concrete and (b) silica-fume-containing concrete.

between the porosity obtained by the MIP and the image analysis (Fig. 2) represents the amounts of finer pores than 0.2 μm. Because the total porosity including the whole range of capillary pores must be greater than the porosity of only coarser pores tallied in the image analysis, the results in Fig. 2 indicate that silica-fume-containing concretes could have more fine pores than concretes without silica fume could.

3.2. Volume fraction of various constituent phases

Fig. 3 shows the volume fractions of various constituents in concretes with and without silica fume. The standard deviation of values measured by the image analysis is given in Table 3. Experimental errors are greater in unhydrated cement than in coarse capillary pores. However, the errors of coarse capillary pores are quite small. It seems that the variations of those measured values are almost comparable to the results of Scrivener et al. [4]. Therefore, the difference in phase constituents between concretes with and without silica fume (Fig. 3) is significant even if the variation of unhydrated cement (i.e., the variation of the degree of hydration of cement) is taken into account.

Reductions in the volume of silica fume due to the reaction are ignored in the calculation of the volume fractions of various phases in the silica fume concretes (Fig. 3b). The volume fractions of hydration products in concretes with silica fume are slightly greater than those in concretes without silica fume at 12 h. However, at 24 h, the ordinary concrete contains more hydration products than the silica fume concrete does. In regard to the pore volume at 24 h, silica-fume-containing concretes exhibited greater capil-

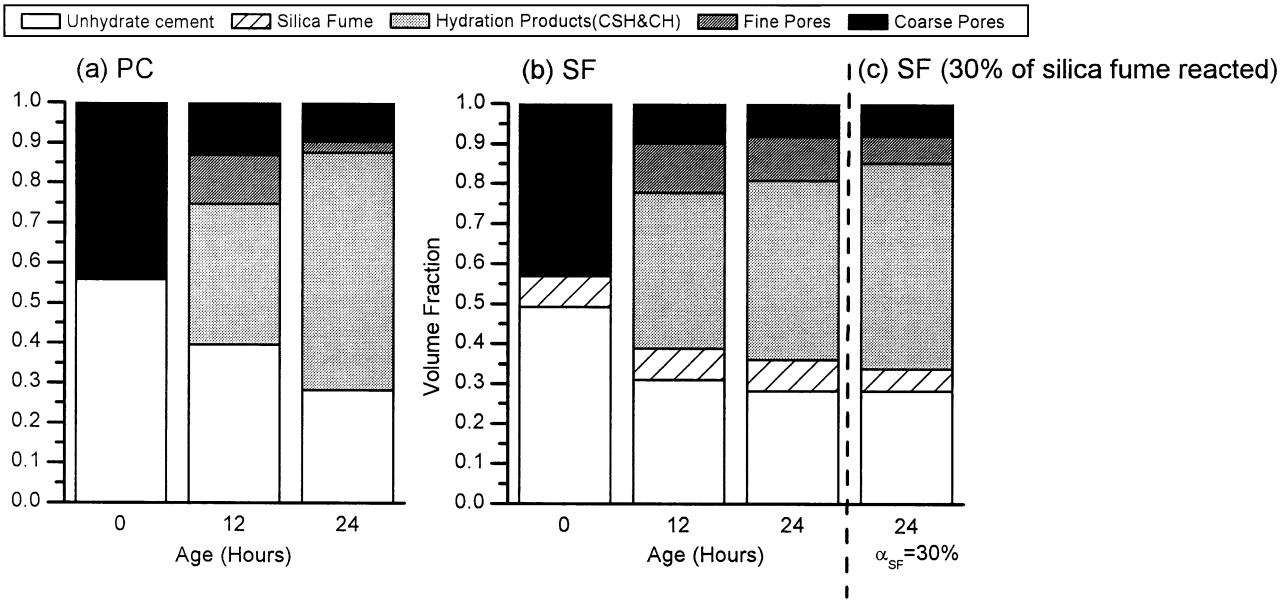

Fig. 3. Volume fractions of constituent phases in concretes (coarse pores: >0.2 μm; fine pores: 0.2 μm–2.5 nm).

Table 3
Standard deviation and coefficient of variation of values measured by image analysis

	Age (h)	Standard deviation (vol.%)		Coefficient of variation	
		Unhydrated cement	Coarse pores	Unhydrated cement	Coarse pores
PC	12	3.0	1.1	0.08	0.09
	24	3.3	0.6	0.12	0.06
SF	12	2.7	0.5	0.09	0.05
	24	3.1	0.5	0.11	0.07

lary porosity of fine pores (<0.2 μm) than ordinary concretes do. However, the amounts of coarse pores have been reduced by the addition of silica fume. The results in Fig. 3 also show that silica-fume-containing concretes have greater numbers of fine pores than do concretes without silica fume at 24 h.

4. Discussion

4.1. Comparison in the total porosity between the MIP and the image analysis

Park et al. [15] have measured the porosity of cement pastes at early ages by the MIP method. According to their results, the total porosity of ordinary Portland cement pastes with a water/cement ratio of 0.25 is about 0.12 and 0.08 cc per unit weight of cement paste at 12 and 24 h of age, respectively. A direct comparison in pore size distributions between all the data obtained by the MIP and the imaging analysis are meaningless. However, if the intrudable pore volume in the MIP method is considered as a comparable index for a given concrete [2] and assumed to be a correct intrinsic value, it is significant to compare the total porosity obtained by the two methods. The total porosities of cement pastes obtained by both methods are given in Table 4. The data determined based on volume in the image analysis were converted to the data based on mass for comparing the results obtained by both methods. In the conversion, the density of hydration product was assumed to be 2.35 g/cm^3 [16]. At the age of 12 h, the porosity estimated by the imaging technique was almost comparable with the value obtained by the MIP method. As for the ordinary concrete at 24 h, only a little difference was found in the porosity between the image analysis and the MIP method. However, there existed a relatively large difference between the values obtained by the image analysis and the MIP method in silica-fume-containing concretes at 24 h. A part of this difference may result from the pozzolanic reaction of silica fume at early ages. However, if it is assumed that silica fume has reacted to some extent, and the pozzolanic reaction is expressed as the following equation [17], it is possible to obtain a modified phase constitution in silica fume concrete at 24 h.

$$S + 1.5\mathrm{CH} + 2.3\mathrm{H} \rightarrow \mathrm{C}_{1.5}\mathrm{SH}_{3.8} \quad (2)$$

where the density of CH is assumed to be 2.24 [16].

The modified phase fractions obtained by assuming that 30% of silica fume has reacted within 24 h are given in Fig. 3c. The mass-based porosity converted from the result of image analysis (Fig. 3c) is consistent with the value obtained by the MIP method (Table 4). Taking into account that considerable amounts of silica fume start to react within 24 h [18], the reaction of 30% of silica fume during the first 1 day seems to be plausible. Thus, the SEM-BSE imaging technique can properly estimate the degree of hydration of cement. The total porosity estimated from the measured amounts of pores by the image analysis, assuming the Powers model, was almost the same as the total porosity measured by the MIP method (Table 4).

Table 4
Comparison between the total capillary porosity obtained by image analysis and the MIP method (cc/g)

		Age=12 h	Age=24 h	Age=24 h
MIP [15]	PC/SF	0.12	0.08	–
Image analysis	PC	0.14	0.07	–
	SF	0.12	0.11	0.08[a]

[a] Assuming that the degree of reaction of silica fume is 30%.

4.2. Effects of characteristics of the pore size distribution on the shrinkage behavior at early ages

As mentioned previously, the difference between the coarse capillary porosity and the total porosity estimated by the image analysis represents the fine capillary porosity (2.5 nm–0.2 μm). Large pores could be connected to gel pores through the fine capillary pores. However, little porosity for fine pores means that large capillary pores detected in the image analysis are isolated so as to be directly connected with gel pores. Comparing bar graphs in Fig. 3a with c, it is found that ordinary concrete has less amounts of fine pores at a given total porosity. Namely, the pore size distribution in ordinary concrete is almost absent in the range of fine pores, i.e., gap graded. In contrast with the discontinuous pore size distribution in the ordinary concrete, the pore size distribution in silica-fume-containing concrete is found to be continuous.

The presence of gap-graded capillary pores in ordinary concretes with an extremely low water/cement ratio of 0.25

may be related to the moisture conditions at early ages. The hydration of cement under such an insufficient water content in the concretes brings about the reduction in relative humidity in concretes even at early ages. Water meniscus was generated in coarse capillary pores so that large empty pores must have been formed in the concretes. Hydration products by subsequent hydration of cement can grow in finer pores containing liquid water, but not in larger empty pores. The characteristic of volume fractions of phases in the concrete with a water/cement ratio of 0.25 (Fig. 3) suggests the occurrence of self-desiccation in the process of hydration of cement at early ages.

As shown in Fig. 3, silica-fume-containing concretes have more fine pores than do concretes without silica fume at 24 h. Little porosity in the range of 2.5 nm to 0.2 μm in concretes without silica fume means that the ordinary concretes have few pores that generate menisci in the range of relative humidity from 0.99 to 0.44. Persson [19] has reported that the relative humidity was reduced by 5–10% for the first 24 h in cement pastes with a water/binder ratio of 0.25. Therefore, the ordinary concrete has less pores that induce the shrinkage due to the capillary tension during the initial decrease in the relative humidity. However, the silica-fume-containing concretes can shrink continuously with time because it contains more pores equilibrium to the decrease in relative humidity. Furthermore, particle sizes of silica fume are approximately the same as those of hydration products [20]. Therefore, silica fume particles can take part in refining capillary pores. Silica fume particles themselves are also involved in forming more fine porous microstructures in concretes with silica fume. Such a refinement of pores by silica fume particles may increase the capillary tension force during the initial decrease in relative humidity. Differences in the autogenous shrinkage between ordinary Portland and silica-fume-containing cement pastes may be partly explained by the differences in capillary pore structures.

5. Conclusions

Pore structures and volume fractions of various constituents in high-strength concretes at early ages were investigated by the BSE imaging technique assuming the Powers model. The major results obtained in this study are as follows:

(1) Coarse capillary porosity in silica-fume-containing concretes was lower than ordinary concretes without silica fume at early ages.
(2) The characteristics of capillary pores in concretes can be estimated by the image analysis method assuming the Powers model for hydration of cement.
(3) At very early ages, most of the capillary pores in ordinary concretes with an extremely low water/binder ratio of 0.25 are so coarse that their pore size distributions were discontinuous.
(4) The pore size distributions in silica-fume-containing concretes were continuous, compared with those in ordinary concretes. The presence of the pores equilibrium to the initial decrease in the relative humidity within concrete may bring about greater autogenous shrinkage in silica-fume-containing concretes.

References

[1] P.-C. Aitcin, The art and science of high-performance concrete, in: P.K. Mehta (Ed.), Proc. Mario Collepardi Symp on Advances in Concrete Science and Technology, CANMET, Ottawa, 1997, pp. 107–121.
[2] S. Diamond, Mercury porosimetry. An inappropriate method for the measurement of pore size distributions in cement-based materials, Cem. Concr. Res. 30 (10) (2000) 1517–1525.
[3] K.L. Scrivener, Microscopy methods in cement paste and concrete, Papers to be presented, but not included in the Proceedings of the 10th International Congress on the Chemistry of Cement, Gorthenburg, Sweden, 1997.
[4] K.L. Scrivener, H.H. Patel, P.L. Pratt, L.J. Parrott, Analysis of phases in cement paste using backscattered electron images, methanol adsorption and thermogravimetric analysis, in: L. Struble, P.W. Brown (Eds.), Microstructural Development during Hydration of Cement, Mater. Res. Soc. Symp. Proc., vol. 85, MRS, Pittsburgh, 1987, pp. 67–76.
[5] K.O. Kjellsen, L. Fjallberg, Measurements of the degree of hydration of cement paste by SEM, 29Si NMR and XRD methods, Proc. Workshop on Water in Cement Paste and Concrete Hydration and Pore Structure, The Nordic Concrete Federation, Skagen, Denmark, 1999, pp. 85–98.
[6] M. Takagi, S. Haruhisa, Handbook of Image Analysis, The University of Tokyo Press, Tokyo, 1991, in Japanese.
[7] D.A. Lange, H.M. Jennings, S.P. Shah, Image analysis techniques for characterization of pore structure of cement-based materials, Cem. Concr. Res. 24 (5) (1994) 841–853.
[8] S. Diamond, M. Leeman, Pore size distributions in hardened cement paste by SEM image analysis, in: S. Diamond, et al., (Eds.), Microstructure of Cement-Based Systems/Bonding and Interfaces in Cementitious Materials, Mater. Res. Soc. Symp. Proc., vol. 370, MRS, Pittsburgh, 1995, pp. 217–226.
[9] T.C. Powers, Physical properties of cement paste, in Proceedings of the 4th International Symposium on the Chemistry of Cement, Washington, DC, vol. 1, 1960, pp. 577–613.
[10] S. Igarashi, M. Kawamura, A. Watanabe, Analysis of cement pastes and mortars by a combination of backscatter-based SEM image analysis and calculations based on the Powers model, Cem. Concr. Compos. (2004) (in press).
[11] J.C. Russ, R.T. Dehoff, Practical Stereology, 2nd edition, Kluwer Academic/Plenum Publishers, New York, 2000.
[12] S. Mindess, J.F. Young, D. Darwin, Concrete, second edition, Prentice Hall, Upper Saddle River, 2003.
[13] M.-H. Zhang, O.E. Gjorv, Effect of silica fume on pore structure and chloride diffusivity of low porosity cement pastes, Cem. Concr. Res. 21 (6) (1991) 1006–1014.
[14] H. Uchikawa, Effect of blending components on the hydration and structure formation of blended cement, Cem. Concr. Cem. Assoc. Jpn. 488 (1987) 33–48 (in Japanese).
[15] K.B. Park, T. Noguchi, F. Tomosawa, A study on the hydration ratio and autogenous shrinkage cement paste, in: E. Tazawa (Ed.), Autogenous Shrinkage of Concrete, Proc. Int. Workshop on Autogenous Shrinkage of Concrete, AUTOSHRINK'98, JCI, Tokyo, 1998, pp. 281–290.

[16] J.F. Young, Hydration of Portland cement, in: D.M. Roy (Ed.), Instructional modules in cement science, Journal of Materials Education, The Pennsylvania State University, PA, USA, 1985, pp. 1–24.
[17] J.F. Young, W. Hansen, Volumetric relationships for CSH formation based on hydration stoichiometries, in: L. Struble, P.W. Brown (Eds.), Microstructural Development during Hydration of Cement, Mater. Res. Soc. Symp. Proc., vol. 85, MRS, Pittsburgh, 1987, pp. 313–322.
[18] Z.-Q. Wu, J.F. Young, The hydration of tricalcium silicate in the presence of colloidal silica, J. Mater. Sci. 19 (11) (1984) 3477–3486.
[19] B. Persson, Self-desiccation and its importance in concrete technology, Mat. Struct. 30 (199) (1997) 293–305.
[20] J.F. Young, S. Mindess, R.J. Gray, A. Bentur, The Science and Technology of Civil Engineering Materials, Prentice Hall, Upper Saddle River, 1998.